Microstructured Polymer Adhesive Feet for Climbing Robots

Kathryn A. Daltorio, Stanislav Gorb, Andrei Peressadko, Andrew D. Horchler, Terence E. Wei, Roy E. Ritzmann, and Roger D. Quinn

Abstract

Novel insect-foot–inspired materials may enable future robots to walk on surfaces regardless of the direction of gravity. Mini-Whegs™, a small robot that uses four wheel-legs for locomotion, was converted to a wall-walking robot with compliant, adhesive feet. First, the robot was tested with conventional adhesive feet. Then a new, reusable insect-inspired adhesive was tested on the robot. This structured polymer adhesive has less adhesive strength than conventional pressure-sensitive adhesives, but it has two important advantages: the foot material maintains its properties for more walking cycles before becoming contaminated, and the feet can then be washed and reused with similar results, which is not feasible with conventional adhesives. After the addition of a tail and widening the feet, the robot is capable of ascending vertical smooth glass surfaces using the structured polymer adhesive.

Introduction

Compact robots are vacuuming household floors, exploring the surface of Mars, inspecting ducts, and performing other tasks that humans find tedious, hazardous, or difficult. Most of these robots are confined to the near-flat surface on which they start. However, if they could climb like insects, tall steep terrain would not be a barrier, and they could access a larger range of environments. If the climbing techniques of robots matched that of geckos, robots might be walking on ceilings, changing high light bulbs, searching collapsed buildings, cleaning building exteriors, or climbing trees for surveillance. For space applications, novel attachment mechanisms may be required to anchor a robot to a surface in the absence of gravity and air pressure.

Already there are robots that can scale various steep substrates; ferrous surfaces can be climbed with electromagnetic effectors.[1] By finding randomly placed handholds, LEMUR II can autonomously climb near-vertical environments.[2] Clean, featureless surfaces can be scaled using suction pads,[3,4] but compressed-air systems are bulky and the speed of the robot is limited by the speed at which the suction cups can be applied and released. Reconfigurable Adaptable MicroRobots[5] are able to traverse a wide range of surfaces by crawling or flipping, but require external power and control to run an onboard suction system. There are surfaces on which suction-based climbing is not effective (e.g., bumpy, perforated, or dirty surfaces), although robots like City Climber[6] overcome some of these issues by maintaining a vortex that generates a low-pressure zone between the robot and the climbing surface.

With greater agility than these climbing robots, a cockroach can climb glass, cardboard, foam, tree bark, and many other substrates. To attach to the smooth surfaces, cockroaches have smooth adhesive pads; to attach to rough and soft surfaces, they have active claws and passive spines.[7] Spinybot is a robot that uses insect-inspired passive spines to ascend rough vertical surfaces.[8]

As already described in this issue of *MRS Bulletin*, beetles, flies, and geckos adhere to surfaces using patches of microscopic hairs (often called fibers or setae) that provide a mechanism for adhesion by van der Waals forces and capillary effects.[9,10] Inspired by these animal mechanisms, new structured adhesives are being developed.[11–13] These adhesives are usually based on the use of either relatively stiff patterned materials, such as a silicon surface, or structured polymers (for details see the articles by Jagota et al. and Chan et al. in this issue). Testing the adhesives on small vehicles is important for understanding insect locomotion as well as for developing versatile robots and improving the performance of the adhesive used for the feet.

Several designs of small adhesive-based climbing robots have been tested with traditional adhesives. Tank-like adhesive treads, rotating spokes tipped with balls of adhesive, and pivoting adhesive plates have been implemented with pressure-sensitive adhesives.[14,15] The resulting robots were able to walk short distances before the adhesive became contaminated.

To improve reliability, observations and experiments on different species of insects provide important inspiration for the kinematics of robot legs. Flies make initial contact with the entire broad, flexible attachment organ (pulvilus).[16] A slight shear component is present in the movement, which provides a preload to the attachment device surface. Shearing of a fibrillar pattern of microstructures along the substrate leads to the bending of single setae and to an increase of the normal load to the substrate. Because single setae of many animal attachment devices bear spatula-like tips, this shear movement also increases the contact perimeter between the setae and the substrate. Similar shearing motion has also been previously described as a part of the attachment mechanism of a single gecko seta.[9] Minimal force expenditure during detachment is also important. Disconnecting the entire attachment organ at once requires overcoming a strong adhesive force, which is energetically disadvantageous. Thus, both flies and geckos peel their feet from the substrate gradually.[9,16]

The principles of contact formation with the entire pad surface and peeling-like

detachment were designed into a Mini-Whegs™ robot with climbing ability (Figure 1). Whegs™ are a series of robots that have a single propulsion motor that drives their multispoke wheel-leg appendages.[17,18] The original Whegs has six wheel-legs, while Mini-Whegs has only four. The spokes allow Whegs robots to climb over larger obstacles than a vehicle with similarly sized wheels. PROLERO[19] and later RHex,[20] both of which preceded Whegs, walk using single-spoke legs driven by separate motors. Their gaits can be adjusted actively by their control systems.

The power-autonomous, radio-controlled robot used in the climbing tests described here is Mini-Whegs7 (5.4 cm × 8.9 cm, 87 g), which has four spokes on each of its four wheel-legs.[21] A foot made of flexible material is bonded to the end of each spoke and acts as a hinge between the foot and spoke. The feet contact the substrate, bend as the wheel-leg turns, peel off the substrate gradually, and spring back to their initial orientation for the next contact. We first demonstrated that this robot could climb glass walls and ceilings using standard pressure-sensitive adhesives (PSAs).[22] However, PSA feet become contaminated with dirt, causing a loss of adhesive properties, and must be replaced often. Next, we investigated a reusable, biologically inspired structured adhesive for the feet of a modified Mini-Whegs to enable it to climb walls.[23]

Biologically Inspired Adhesives

We tested two polymer samples, one with a smooth flat surface and the other with a biologically inspired surface structure (Figure 2). Both samples are made of two-compound, polymer poly(vinyl siloxane) (PVS).[11] This polymer was chosen for its excellent molding properties and low surface energy. The Young's modulus E of the bulk polymer is 2.5–3 MPa.[13] The surface energy was calculated according to the method of Wu[24] from the contact angles of distilled water, diiodomethane, and ethylene glycol measured with an OCA-20 contact angle measurement device (Dataphysics GmbH). PVS is a highly hydrophobic material, and the contact angle of distilled water on its surface was 112°. The surface energy of PVS was 16.1 mJ/m^2 (dispersion component γ_d = 13.1 mJ/m^2, polar component γ_p = 3 mJ/m^2). The smooth samples (thickness, 0.4 mm) were molded from a clean glass surface. The structured samples were obtained from the company Gottlieb Binder GmbH & Co. KG. The base thickness of the structured sample was approximately 0.4 mm. The protrusions were about 100 μm high and about 40 μm in diameter. The structure was inspired by our previous work on insects.[10,11] The shape and size of the outgrowths were similar to those described in male beetles from the family Chrysomelidae, which demonstrate excellent adhesive properties.

The tangential forces (i.e., traction) were compared for 15-mm-wide × 35-mm-long samples of the flat and structured PVS material attached to a steel needle. A 10.5-cm-long thread connected the protruding ends of the needle to the force sensor. At a constant speed of 1.47 mm/s, the samples were pulled along flat smooth glass that was first cleaned with alcohol and deionized water and dried with a nitrogen jet. Forces were measured with a piezoelectric force transducer (FORT 1000 combined with an electric control system ADC MP100) and force–time data were transferred to a computer, visualized, and processed with AcqKnowledge 3.7.2 (BIOPAC Systems Inc.). Typical force–time plots for the flat and structured surfaces are shown in Figures 3a and 3b, respectively. The flat sample exhibits typical stick-slip behavior with a maximum force of 1300 mN and zero minimal force. In contrast, the mean traction force for the structured sample is 530 mN (standard deviation, 41 mN), and the maximal force is 600 mN.

Traction between the flat sample and the substrate is very sensitive to even the

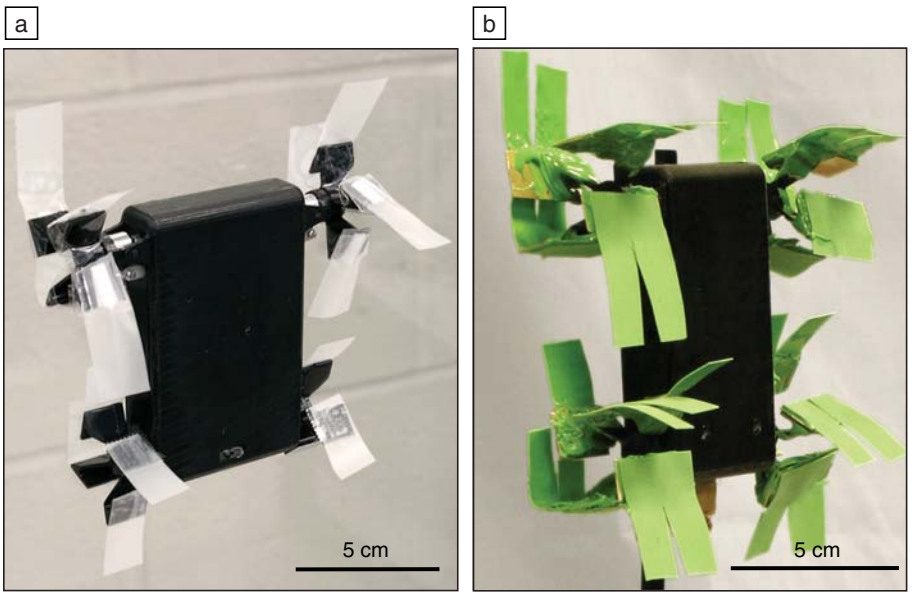

Figure 1. Mini-Whegs7™ (5.4 cm × 8.9 cm, 87 g) on vertical glass (a) with adhesive tape feet and (b) with poly(vinyl siloxane) microstructured polymer feet and 25-cm-long tail (not shown).

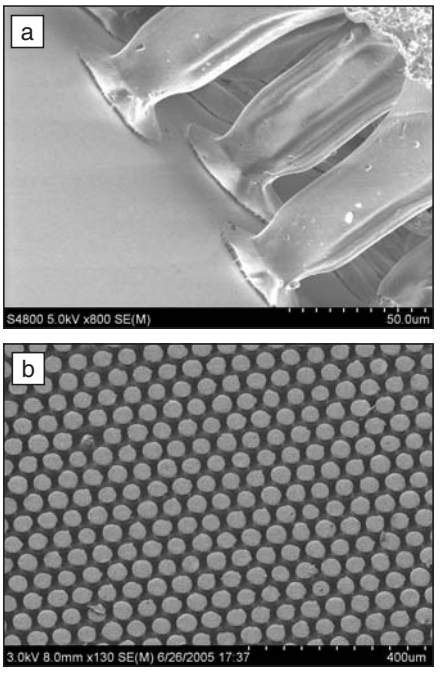

Figure 2. Scanning electron microscopy images of the structured adhesive used in the experiments described in this article. (a) Single microstructures of the structured poly(vinyl siloxane) (PVS) surface in contact with the glass surface. (b) Structured PVS surface viewed from above, showing the hexagonal pattern of microstructures.

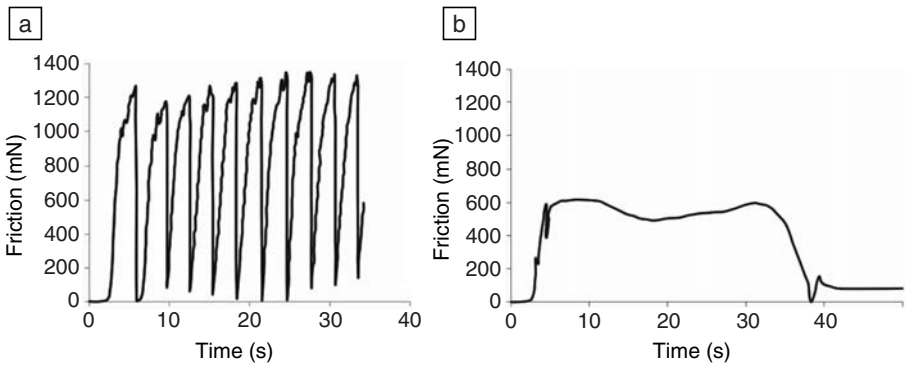

Figure 3. Traction test results for (a) flat and (b) structured polymer samples. The flat sample shows a strong stick-slip, whereas the structured sample demonstrates rather smooth sliding.

slightest contamination. After a series of 3–4 trials, the flat sample produced little traction, while the structured sample could be tested repeatedly, losing friction only after hundreds of cycles. Cleaning with water recovers the traction ability of both samples. In summary, the structured material has a lower maximum traction force, but has the advantages of not exhibiting stick-slip and being less sensitive to contamination.

To characterize the adhesive properties, peel testing was performed. Peeling is the delamination of a thin film from the substrate under action of a loading force F acting under an angle θ to the substrate. In the experiment, the peeling force needed for delamination of the polymer adhesive (flat and structured) was measured.

Flat and structured PVS samples (25 mm wide) were attached to a clean smooth glass surface in a horizontal position and loaded with a weight. Then, the tilt angle of the glass was increased by steps of 2.5° until peeling was observed (Figure 4a). The normalized equilibrium force F/b was plotted versus the peeling angle θ (Figure 4b). The Kendall model of peeling was applied to estimate the adhesion energy:[25]

$$\left(\frac{F}{b}\right)^2 \frac{1}{2Ed} + \left(\frac{F}{b}\right)(1-\cos\theta) - R = 0, \qquad (1)$$

where F is the peeling force, d is the thickness of the adhesive, b is the width of the tape, E is the elastic modulus of the film material, θ is the peeling angle, and R is the energy required to fracture a unit area of an interface. The adhesion energy R for the structured material was 0.90 J/m^2 and 0.49 J/m^2 for the flat material. These tests demonstrated that structuring does benefit the polymer's adhesion at this range of peeling angle. Similar testing of new Scotch® adhesive tape yields approximately 10 times the adhesion energy of the structured polymer. While the structured polymer does not have the adhesive strength of Scotch tape, the polymer has advantages in that it does not become contaminated quickly and can be washed.

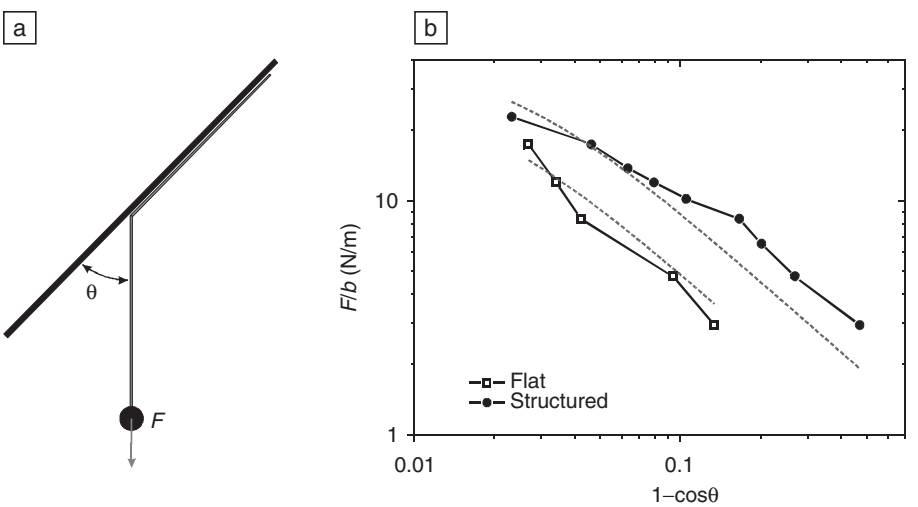

Figure 4. (a) Diagram of the peeling experiment. (b) Normalized equilibrium force, F/b, versus peeling angle, θ, for flat and structured materials. Dashed lines indicate fit corresponding to Kendall's model of peeling.[25]

Robotic Climbing Failure Modes

There are two fundamental modes of failure for a surface-climbing robot. First, the robot can slip along the substrate because of insufficient tangential (traction) forces. Second, there may be insufficient normal (adhesive) forces, causing the robot to tumble away from the wall. Support behind the rear axle (e.g., a tail) can reduce the likelihood of tumbling while increasing the tendency of slipping.

The vehicle falls backward from the wall when the feet on the front axle are not tenacious enough to support the normal force, N_1, required to balance the moment of the weight. By summing moments about the rear foot contact point (Figure 5a), the mag-

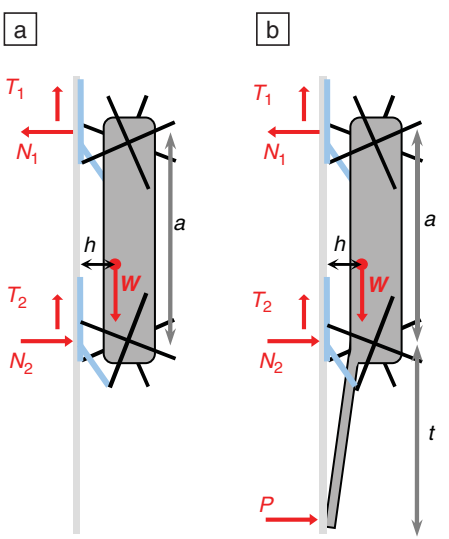

Figure 5. Free-body diagrams of (a) robot without tail and (b) robot with tail on vertical surface. Forces on the robot are shown as red arrows. N is normal forces, T is tensile force, W is the weight, a is the wheelbase, and h is the leg length.

nitude of N_1 for a vehicle without a tail of weight W is

$$N_{1_{\text{No Tail}}} = \frac{hW}{a} \text{ (tensile)}. \quad (2)$$

Therefore, 0.23 N of normal force is required to support the 87 g robot with a wheelbase of 7 cm and leg length of 1.9 cm. Because the supportable normal force decreases with peeling angle, the critical position occurs when the wheel hub on one side has just peeled up one foot and has not yet applied the next foot. At that instant, the foot on the other side of the axle must be capable of supporting the moment of the robot's weight. Otherwise, the robot will rotate away from the wall, inhibiting proper foot placement. Because the feet are 4° out of phase, this should occur when the foot currently peeling is parallel to the substrate. A video of the robot with PSA feet shows that the average peeling angle at that instant is 60° (SD = 5°, number of measurements n = 6). Using Equation 1, the force per unit width for the structured polymer is 0.018 N/cm. The component in the normal direction is 0.016 N/cm, which would require the feet to be at least 14 cm wide.

However, if a tail is added, the normal force P at the tail/wall contact point can aid the adhesive in countering the moment of the weight. By summing the moments about the rear foot contact point (Figure 5b), the required adhesive force from the front feet is

$$N_{1_{\text{With Tail}}} = \frac{hW - tP}{a} \text{ (tensile)}, \quad (3)$$

where t is the length of the tail. Thus, a robot with a tail will require less normal force to prevent it from tumbling backwards on a substrate, assuming a lightweight tail.

The disadvantage of the tail is that it tends to decrease the traction forces that prevent the robot from slipping. For most interfaces, the tangential forces are largest when the normal forces are most compressive. For the robot without a tail, the rear normal force, N_2, will always be equal and opposite the front normal force, N_1 (as given in Equation 2):

$$N_{2_{\text{No Tail}}} = \frac{hW}{a} \text{ (compressive)}. \quad (4)$$

For a robot with a tail, the sum of the forces N_1 and N_2 must be equal and opposite to P, and from Equation 3:

$$N_{2_{\text{With Tail}}} = \frac{hW - (a+t)P}{a} \text{ (compressive)}. \quad (5)$$

Thus, N_2 with a tail is always less than without a tail. If the tail is long and stiff enough, N_2 can actually be in tension. Reducing the contact force decreases the available traction, which may cause the robot to slip.

Robot Performance

The performance with Scotch tape demonstrates the potential of future adhesive climbing robots. With tape, no tail was needed and the robot (87 g) was able to climb reliably enough to test steering, obstacle climbing, and ceiling walking. The vehicle walked up, down, and sideways on vertical planes of glass using Scotch tape feet. Further, the robot walked inverted across the underside of a 30-cm-long horizontal surface. The vehicle also demonstrated successful transitions from the floor to a vertical wall and from a wall to the floor. Currently, it is possible to steer the robot while it is climbing on a vertical surface but only gradually. In a test to demonstrate climbing distance, the robot ascended a 70 cm vertical surface four consecutive times at a speed of 5.8 cm/s without falling—a total of 280 cm. Afterwards, the robot fell with increasing frequency as the tape became dirty or damaged.[22]

After the 1.6-cm-wide tape was replaced with pieces of structured PVS adhesive of the same size and the batteries were moved off-board, the 76 g robot was able to climb an incline of 50° but fell backwards from the substrate at higher angles. The batteries were removed to reduce weight and thereby reduce the amount of attachment force that was needed. Power for the drive motor was provided off-board. By adding a 6.6 cm tail and widening the front feet to 2.6 cm, the robot (at 110 g) was able to scale a 60° incline reliably. It scaled the entire length of the incline (39 cm) at a speed of 8.6 cm/s. The robot made 13 similar-length runs without falling and without requiring washing. Reversing the driving direction on the wall resulted in the robot falling and then catching itself on the substrate.[26]

By lengthening the tail to 25 cm and widening the back feet to 2.6 cm, the robot (at 132 g) was able to climb a vertical glass surface (see Figure 1b). With the longer tail and widened feet, the robot could be placed on a vertical surface and rest indefinitely. However, walking on the vertical surface was less reliable than with the tape: the robot slid or lost traction on the substrate in 44% of the trials (n = 16). In the trials in which the robot did make forward progress, the robot walked an average of 18 cm. The longest walk was 58 cm (the entire length of the surface) at 2.3 cm/s. The structured PVS feet retained their traction and adhesive properties for several hours of testing and could be renewed by washing with soap and water.[26]

Future Improvements

Mini-Whegs can walk for short distances on clean glass walls and ceilings using PSA feet because of the strong adhesive properties of the PSA. However, within minutes, the PSA becomes contaminated, preventing the robot from climbing further. The structured PVS material used in this research produces an order of magnitude less adhesive force per unit area than PSAs, but is more resistant to contamination and can be cleaned and reused for hours. After a tail was added, the robot with structured PVS feet could climb a vertical wall.

The ability to transition between orthogonal surfaces, steer, and overcome small obstacles is feasible for a robot with compliant adhesives, as demonstrated by trials in which Scotch tape was used. A lighter robot would require less adhesion, making it easier for the robot to stay affixed to the substrate and allowing for more complex maneuvers. In addition, a lighter robot may not need a tail, which can get in the way during transitions between surfaces of different inclinations. With a body flexion joint, as observed in various walking animals, the robot might even be able to make transitions around more difficult external angles.[27] The addition of anisotropic frictional material on the lower tail surface, where the normal forces are compressive, may reduce the tendency of the robot to slip down the substrate. Some geckos have adhesive tails[28] that may provide similar function.

Whereas the current robot is only able to walk vertically on clean smooth surfaces, a practical climbing robot would need to be able to traverse other surfaces as well. To achieve this, sharp claws or insect-like spines could be added to penetrate soft substrates or catch on asperities. The combination of different attachment mechanisms is common among insects and geckos. The robot Spinybot has already demonstrated that arrays of properly applied spines can take advantage of surface roughness to hold a robot on stucco and concrete walls.[8] When combining multiple attachment mechanisms on the same robot, it is important that the adhesive not become contaminated on these other surfaces. In addition, the application of the different attachment mechanisms must not interfere with each other. On Mini-Whegs, adding a pair of sharp metal spines to the feet enables the robot to climb steep (up to 60°) inclines of

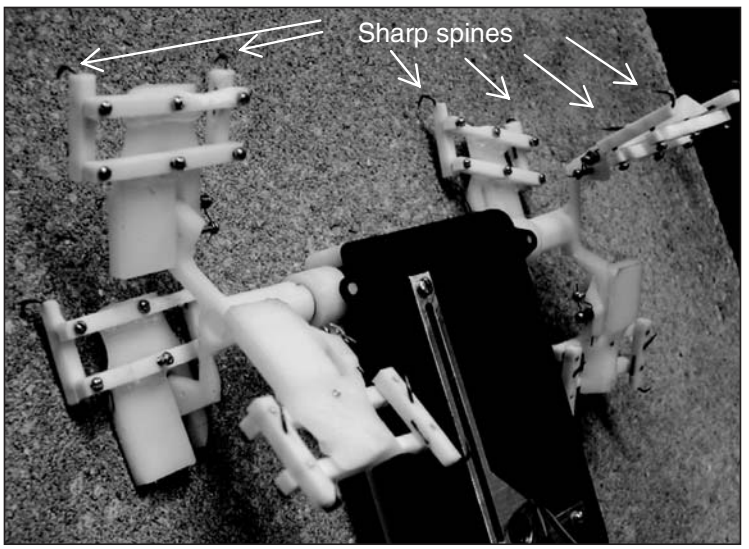

Figure 6. Climbing Mini-Whegs (5.4 cm × 8.9 cm) scaling rough concrete with sharp spines. Scotch® tape or another adhesive, not pictured, can be added to similar wheel-legs such that the robot can scale both smooth and rough surfaces.

glass, Styrofoam, or rough concrete[23] (Figure 6).

Acknowledgments

This work was supported by NSF/IGERT grant DGE-9972747, NDSEG, Zonta International, the National Geospatial Intelligence Agency contract C0N030858 and U.S. Air Force contract F08630–03–1-0003, and the Federal Ministry of Research of Education Germany (BMBF) InspiRat grant 01RI0633.

References

1. L. Guo, K. Rogers, R. Kirkham, in *Proc. Int. Conf. on Robotics and Automation* Vol. 3 (IEEE, San Diego, CA, 1994) pp. 2495–2500.
2. T. Bretl et al., in *Proc. Int. Symp. on Experimental Robotics* (ISER, Singapore, 2004).
3. S. Hirose, K. Kawabe, in *Proc. Int. Conf. on Walking and Climbing Robots* (CLAWAR, Brussels, Belgium, 1998).
4. T. Yano, T. Suwa, M. Murakami, T. Yamamoto, in *Proc. Int. Conf. on Intelligent Robots and Systems* (IROS, Grenoble, France, 1997) pp. 249–254.
5. R. Lal Tummala et al., *IEEE Robotics and Automation Magazine* **9**, 10 (December 2002).
6. J. Xiao, W. Morris, N. Chakravarthy, A. Calle, *Proc. SPIE* **6230**, 62301 (2006).
7. S.F. Frazier et al., *J. Comp. Physiol. A* **185**, 157 (1999).
8. K. Sangbae, A.T. Asbeck, M.R. Cutkosky, W.R. Provancher, in *Proc. Int. Conf. on Advanced Robotics* (ICAR '05, Seattle, WA, 2005) pp. 601–606.
9. K. Autumn et al., *Nature* **405**, 681 (2000).
10. M.G. Langer, J.P. Ruppersberg, S. Gorb, in *Proc. R. Soc. London, Ser. B* **271**, 2209 (2004).
11. S. Gorb, M. Varenberg, A. Peressadko, J. Tuma, *J. R. Soc. Interface* **4**, 271 (2006).
12. A.K. Geim et al., *Nature Mater.* **2**, 461 (2003).
13. A. Peressadko, S.N. Gorb, *J. Adhes.* **80**, 247 (2004).
14. C. Menon, M. Murphy, M. Sitti, in *Proc. IEEE ROBIO '04* (Shenyang, China, 2004).
15. "Unlocking the Secrets of Animal Locomotion," University of California, Berkeley, Press Release, www.berkeley.edu/news/media/releases/2002/09/rfull/robots.html (accessed May 2007).
16. S. Niederegger, S. Gorb, *J. Insect Physiol.* **49**, 611 (2003).
17. R.D. Quinn et al., *Int. J. Robotics Res.* **3**, 169 (2003).
18. R.D. Quinn, D.A. Kingsley, J. Offi, R.E. Ritzmann, in *Proc. Int. Conf. on Intelligent Robots and Systems* (IROS '02 Lausanne, Switzerland, 2002) pp. 2652–2657.
19. A. Martin-Alvarez et al., in *Proc. 2nd World Automation Congress* (WAC '96, Montpellier, France, 1996).
20. U. Saranli, M. Buehler, D. Koditschek, *Int. J. Robotics Res.* **20** (7), 616 (2001).
21. J.M. Morrey et al., in *Int. Conf. on Intelligent Robots and Systems* (IROS '03, Las Vegas, USA. 2003) pp. 82–87.
22. K.A. Daltorio et al., in *Int. Conf. on Intelligent Robots and Systems* (IROS '05, Edmonton, Canada, 2005) pp. 3648–3653.
23. T.E. Wei et al., in *Int. Conf. on Climbing and Walking Robots (CLAWAR '06,* Brussels, Belgium, 2006).
24. S. Wu, *J. Polym. Sci.* **C34**, 19 (1971).
25. K. Kendall, *J. Phys. D: Appl. Phys.* **8**, 1449 (1975).
26. K.A. Daltorio et al., in *Proc. Int. Conf. on Climbing and Walking Robots* (CLAWAR '05, London, 2005).
27. R.E. Ritzmann, R.D. Quinn, M.S. Fischer, *Arthropod Struct. Dev.* **33**, 361 (2004).
28. A.M. Bauer. *J. Morphol.* **235**, 41 (1998). □